PERGAMON

European Polymer Journal 35 (1999) 923–937

EUROPEAN POLYMER JOURNAL

Molecular mobility in polyurethane/styrene–acrylonitrile blends studied by dielectric techniques

A. Kanapitsas [a], P. Pissis [a,*], A. Garcia Estrella [b]

[a] *National Technical University of Athens, Department of Physics, Zografou Campus, 15780 Athens, Greece*
[b] *Department of Applied Thermodynamics, Universidad Politecnica de Valencia, Valencia, Spain*

Received 28 May 1997; accepted 13 January 1998

Abstract

We report in this work the results of dielectric studies on microphase separation in blends of thermoplastic polyurethanes (TPUs) and styrene–acrylonitrile (SAN) copolymers with 0, 25, 50, 90 and 100% SAN (w/w). The dielectric techniques used include broadband ac dielectric relaxation spectroscopy (DRS), in the frequency range of 10^{-2} to 10^{7} Hz and a temperature range of 20–200°C, and thermally stimulated depolarization currents (TSDC) techniques in the temperature range of −170–30°C. These techniques enable us to observe the primary α relaxations and the secondary γ and β relaxations of TPU and SAN in the pure components and in the blends and to follow the dependence of their characteristic parameters on composition. DRS proves to be very sensitive in monitoring the melting of the crystalline soft segments of TPU in the blends. In addition the investigation of dc conductivity effects in the blends provides information on the morphology of the blends at mesoscopic level. The results suggest that the extent of partial miscibility of the two components is very limited, whereas the addition of SAN in TPU promotes the separation of hard and soft segments in TPU.

1. Introduction

Recently scientific interest in polymer blends has intensified [1–3]. Polymer blends give the possibility to combine contrary properties of different polymeric materials, the range of behaviour combinations being higher than that achieved by copolymerization. Thus, blending of polymers is an effective way of producing advanced multicomponent polymeric systems with new property profiles [3, 4]. From the fundamental point of view, polymer blends are interesting systems for studying polymer interactions and phase separation at microscopic and mesoscopic levels [1–4].

Polyurethane-based blends generally have an added thermoplastic hard component to improve their mechanical properties [5]. These blends are widely used for many technological applications and their properties are being intensively investigated. The blending of thermoplastic polyurethane (TPU) with polystyrene-co-acrylonitrile (SAN) results in many property variations due to the numerous combinations of different polyurethane types (hard and soft segment character, domain separation, etc.) with different SAN copolymers (weight % of acrylonitrile and different distributions of styrene and acrylonitrile) that are possible [6–9]. The chemical structure of TPU/SAN blends is, in general, very complex [6, 9].

The present work deals with the investigation of molecular mobility and microphase separation in TPU/SAN blends by means of dielectric methods. The composition of the blends studied was varied in a broad range from pure TPU to pure SAN. The dielectric methods used included broadband a.c. dielectric relax-

* Corresponding author.

0014-3057/99/$ - see front matter
PII: S0014-3057(98)00075-5

ation spectroscopy (DRS) in wide ranges of frequency, 10^{-2}–10^{7} Hz, and temperature, 20–200°C, and thermally stimulated depolarization currents (TSDC) techniques in the temperature range of −170–30°C. DRS and TSDC have proved very effective in investigations of molecular mobility and structure–properties relationships in polymeric blends [2–4, 10, 11]. They make it possible for primary α relaxations and the secondary γ and β relaxations of TPU and SAN to be studied and changes in their dynamics induced by blending followed.

The results of DRS measurements are analysed within the complex permittivity ε^* and the complex modulus M^* formalism [12]. For ion conducting systems the M^* formalism offers several advantages: the space charge effects often do not mask the features of the spectra (highly capacitive phenomena are suppressed in the frequency plots of the imaginary part of M^*, M'' (f)); the M'' (f) spectra show peaks which are related to the ionic conductivity and their peak frequencies show the same temperature dependence as the dc conductivity (conductivity current relaxation [13]). Depending on temperature and frequency of DRS measurements, charge carriers move over distances of variable length. Thus, detailed investigations of conductivity effects are carried out within this work to obtain information on the morphology at the mesoscopic level. Finally, temperature plots of the real permittivity ε' at a suitably fixed frequency are employed to monitor phase transitions involving dipolar components, such as the melting of the crystalline soft segments of TPU and the glass to rubber transition of the hard segments of TPU in the blends.

2. Experimental

2.1. Materials

The TPU/SAN samples were a gift from the University of Maribor. TPUs were synthesized from poly(caprolactone) (CAPA) $M_n = 2000$, 4,4′-methylenediphenyl diisocyanate (MDI) and 1,2-propanediol by a standard prepolymer process. Commercial SAN (Luran 388 S, BASF, acrylonitrile content 32.9 wt%) was used for blending with TPU. Polymers were blended in solution: TPU and SAN in ratios of 100/0, 75/25, 50/50, 10/90 and 0/100 were dissolved in dimethylformamide (DMF) at room temperature in 15 wt% concentration. From the solution, films were cast and dried in a vacuum at 40°C for 6 h. The temperature of drying was limited to 40°C because of melting of the crystalline soft segments of TPU at higher temperatures [9]. The thickness of the films was approximately 30 μm.

For comparison, some measurements were performed with a second blend, labelled PUR/SAN, the main difference to TPU/SAN being that in PUR/SAN the SAN copolymer was synthesized in the laboratory. Cross-linked polyurethanes were prepared by the one-shot technique from a polypropylene glycol with 15% ethylene oxide termination ($M_n = 3500$, functionality 2.8), MDI and 1,4-butanediol. SAN was synthesized in the polyol from styrene, acrylonitrile and azoisobutyronitrile as an initiator. Blends with 10 and 20 wt% SAN were prepared. For details of preparation refer to ref. [14].

2.1.1. Dielectric relaxation spectroscopy (DRS) measurements

For a.c. dielectric relaxation spectroscopy measurements two different experimental set-ups were used. In the frequency range 10^{2}–10^{7} Hz and the temperature range of 20–200°C a Hewlett–Packard HP4192A Impedance Analyser combined with the Ando type TO-19 thermostatic oven and the Ando SE-70 dielectric cell, with nickel-coated stainless steel electrodes, were used. A Schlumberger Frequency Response Analyser (FRA 1260), supplemented by a buffer amplifier of variable gain and a Novocontrol sample holder with gold-coated electrodes (BDS 1300) were used for measurements in frequency in the region 10^{-2}–10^{6} Hz at 30°C. Complex admittance measurements were performed in a two-terminal electrode configuration. In addition, d.c. conductivity was measured by means of a Hewlett–Packard HP4339 High resistance meter.

2.1.2. Thermally stimulated depolarization current (TSDC) measurements

The TSDC method consists of recording the thermally activated release of frozen-in polarization and corresponds to measuring dielectric losses vs temperature at low frequencies in the range 10^{-4}–10^{-2} Hz [15]. A brief description of the technique is given in the following. The sample is inserted between the plates of a capacitor, made of brass, and polarized by the application of a field E_p at a temperature T_p for a time t_p which is large compared with the relaxation time at T_p of the dispersion under consideration. With the electric field still applied the sample is cooled down to a temperature T_0 sufficiently low enough to prevent depolarization by thermal agitation. Next it is short-circuited and reheated at a constant rate b. A discharge current is generated as a function of temperature which is measured with a sensitive electrometer. The resultant TSDC spectrum often consists of several peaks whose shape and location are characteristic of the relaxation mechanisms of the sample. The analysis of the shape of the TSDC curve makes it possible to obtain the activation energy E, the pre-exponential factor τ_0 and the contribution $\Delta\varepsilon$ of a peak to the static permittivity.

We used a home made experimental apparatus for TSDC measurements in the temperature range of −170–30°C [16]. For details of TSDC measurements and analysis refer to refs [16, 17].

3. Results and discussion

3.1. TSDC measurements

Fig. 1 displays the TSDC thermogram measured on a TPU/SAN blend with 50% SAN. The TSDC spectra from all the samples exhibit the structure shown in Fig. 1. Three dispersion regions are well discerned γ, β, α in the order of increasing temperature. Fig. 2 shows the low temperature region of the TSDC thermograms with the γ and β dispersions for the pure components and the 50/50 TPU/SAN. In pure TPU the γ peak is located at about −155°C and the β peak at about −110°C. The γ peak, which has also been observed in mechanical relaxation spectroscopy on polyurethanes [18], has been associated with local motion of $(CH_2)_n$ sequences [18, 19]. The β peak is attributed to the motion of the polar carbonyl groups [20]. This peak has been found to shift to higher temperatures and to increase in magnitude with moisture, suggesting an association of the adsorbed water molecules with the carbonyl groups [20]. The mechanical β peak, which shows the same moisture dependence, is located at higher temperatures [20]. In pure SAN the γ peak is located at about −165°C and the β peak at about −135°C. Consistent with results obtained with many polymeric systems [18, 19] and with respect to the structure of SAN [21, 22], we attribute the γ peak to local motions of $(CH_2)_n$ sequences and the β peak to motions of the highly polar -CN side group attached to -C in the main chain of SAN.

In the blends the γ and β peaks were found to be located at temperatures between those of the corresponding peaks in the pure components and to systematically shift to lower temperatures with increasing SAN content, (at about −160 and −120°C in 50/50 TPU/SAN blend in Fig. 2). The magnitude of the peaks was found to be between those of the pure components and to increase, in general, with increasing SAN content. These results suggest that the secondary mechanisms of SAN are antiplasticized in the blends (i.e. they shift to higher temperatures), whereas those of the TPU are plasticized (i.e. they shift to lower temperatures).

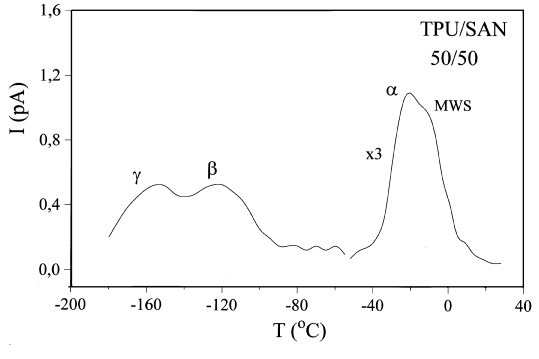

Fig. 1. TSDC thermogram measured on a 50/50% TPU/SAN sample.

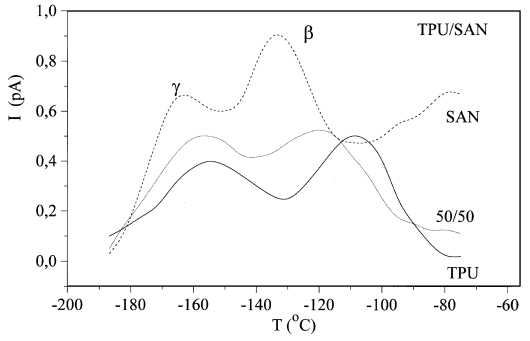

Fig. 2. Low temperature TSDC spectra of pure SAN, pure TPU and 50/50 TPU/SAN blend.

The double peak in Fig. 1 at about −20°C was observed in pure TPU and in the blends. In agreement with the results of measurements in many polyurethane systems the double peak is associated with the glass–rubber transition of the TPU rich phase and the Maxwell–Wagner–Sillars (MWS) interfacial peak, which appears as a shoulder on the high temperature side of the α peak [10, 20]. The α relaxation peak is due to the reorientation of the polar soft segments of the chain during the glass transition of the TPU, whereas the MWS peak is due to the polarization at the interfaces between soft and hard segments of the sample [10, 20]. In our blends the double peak was found to shift slightly but systematically to lower temperatures with increasing SAN content. The α peak shifts from −18°C for pure TPU to −33°C for the 10/90 TPU/SAN blend (Fig. 3). The peak temperature of the TSDC peak associated to the glass transition has been found to be a good measure of the calorimetric glass transition temperature T_g [10, 20]. Thus, the results in Fig. 3 indicate that the glass transition temperature T_g of the TPU rich phase is slightly plasticized in the blends. These results are in excellent agreement with those of DSC measurements on the same blends [23]. The normalized magnitude, I_n, of the double peak decreases systematically with increasing SAN content (Fig. 3). The normalized magnitude of a TSDC peak, defined as the current maximum (current

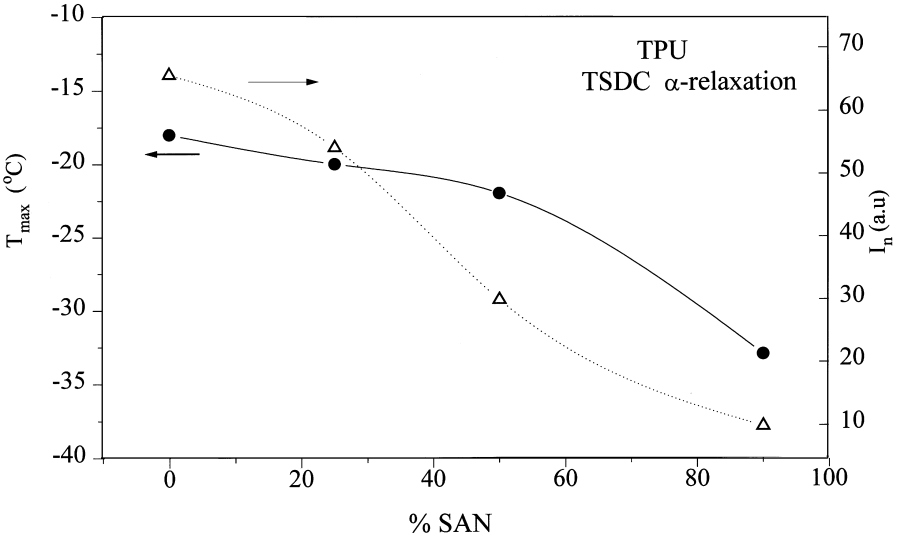

Fig. 3. Position in the TSDC spectrum (maximum current temperature T_m) and strength (normalized maximum current, I_n) of the α-relaxation peak of TPU rich phase, as a function of composition in blends.

at peak temperature, divided by heating rate b, surface area of sample and polarizing field E_p, is proportional to the number of relaxing units contributing to the peak [15–17]. Thus, the decrease of I_n with increasing SAN content is in agreement with our interpretation for the origin of the double peak in TPU and in blends.

The plasticization of the γ, β and α relaxations of TPU and the antiplasticization of the γ and β relaxations of SAN (as well as of the α relaxation in the DRS measurements to be reported in the next section) cannot be explained based on phase composition [6–9] (and even if they were miscible SAN should be plasticized, not TPU). A plausible explanation for the observed behaviour is that these effects are produced by redistribution of low molecular weight oligomers contained in the commercial SAN used. These oligomers act as plasticizers for the SAN used. When the blend is prepared by melt blending or casting from a common solvent a part of these oligomers moves to the second component of the blend (TPU phase here) with the result that the transition temperatures for both the secondary and the primary (α) mechanisms decrease. At the same time due to the smaller amount of plasticizer in the SAN phase the transition temperatures for the primary (α) and the secondary (γ, β) mechanisms increase. Similar effects were observed on other systems based on commercial SAN, e.g. on blends of polycarbonate with acrylonitrile–butadiene–styrene materials [21] and on acrylonitrile–butadiene–styrene graft copolymers [22]. The styrene and acrylonitrile oligomers were isolated and characterized [21] and the explanation for the observed effects was tested by repeating the experiments with purified SAN materials [21, 22]. In several commercial SAN samples analysed the total amount of oligomers was found to be 1–2 wt% [22]. The oligomers were found to be mostly trimers containing two acrylonitrile units and one styrene unit [21]. We may assume that similar holds for the commercial SAN used in this work.

In order to check the hypothesis that the observed plasticization of TPU and antiplasticization of SAN in the TPU/SAN blends is due to migration of oligomers present in the commercial SAN used, TSDC (and DRS) measurements were performed on the PUR/SAN system based on synthesized SAN. Unpolymerized monomers were removed from that system via a rotary evaporation [14]. Fig. 4 shows

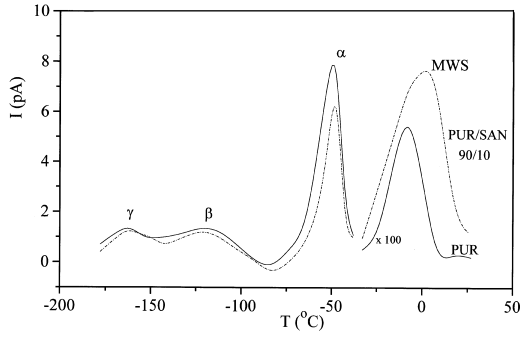

Fig. 4. TSDC thermograms measured on PUR (-) and on PUR/SAN with 10 wt% SAN (- - -).

TSDC thermograms measured on a PUR sample and a PUR/SAN sample with 10 wt% SAN. We observe that both secondary (γ, β) and the primary (α) transitions of PUR are slightly shifted to higher temperatures (antiplasticized) and that only the interfacial MWS relaxation is significantly influenced by addition of SAN. Similar results were obtained with a sample of 20 wt% SAN. These results (to be confirmed by DRS measurements in the next section) suggest that the extent of partial miscibility is very limited and confirm that the large transition temperature shifts observed with the TPU/SAN blends result from partitioning between the phases of oligomers in the commercial SAN copolymer.

3.2. DRS measurements

In Fig. 5 we show results on TPU/SAN blends from dielectric relaxation spectroscopy (DRS) measurements. Fig. 5(a) shows frequency spectra of the real

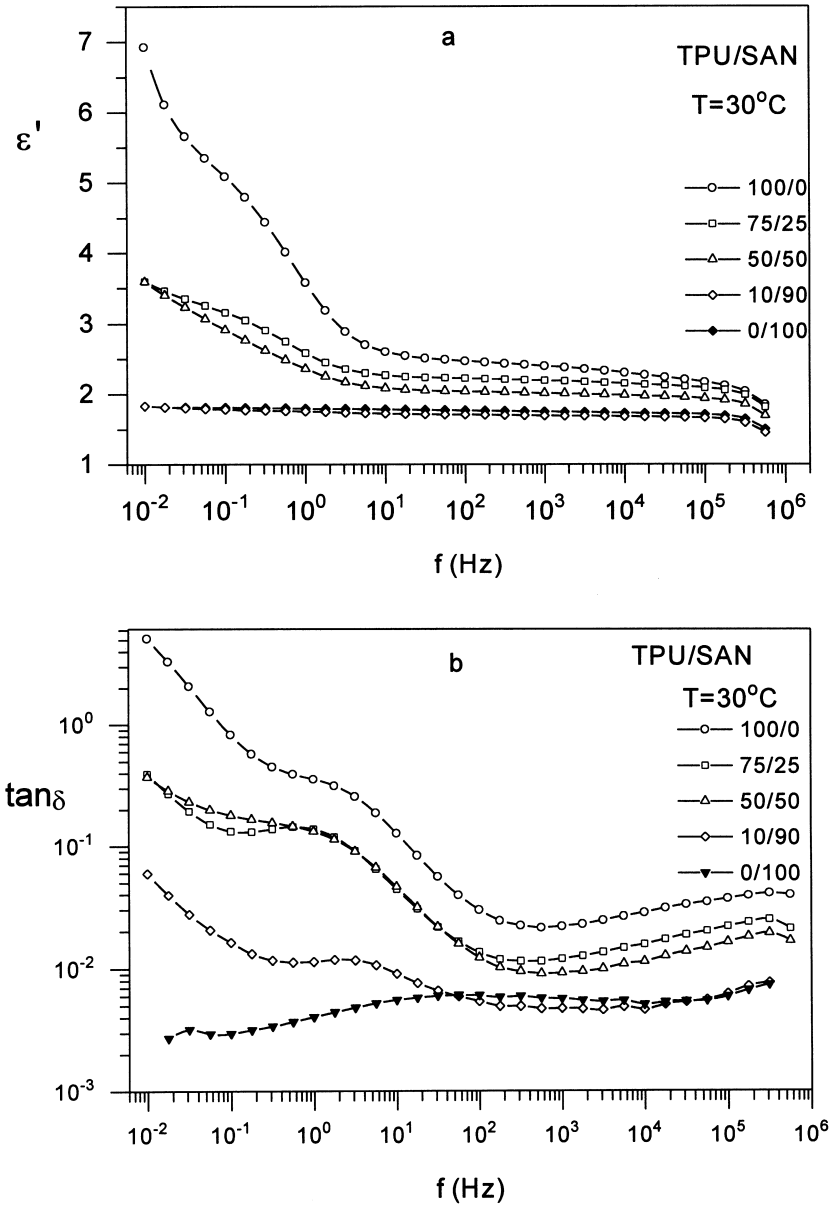

Fig. 5. Dielectric permittivity ε' (a) and dielectric loss tangent $\tan\delta$ (b) as a function of frequency f for the TPU/SAN blends measured at $T = 30°C$.

part ε' of the complex dielectric function ε^* (f, T) = $\varepsilon' - i\varepsilon''$ for pure TPU, pure SAN and TPU/SAN blends at $T = 30°C$. In Fig. 5(b) we show spectra of the dielectric loss tangent (tan $\delta = \varepsilon''/\varepsilon'$, ε'' the imaginary part of ε^*) for the same samples as in (a). The dispersion in the high frequency region of the spectra ($f \approx 10^4$ Hz) for the pure TPU sample and the blends is due to the glass–rubber transition of the TPU soft segments phase. This is the dispersion we studied in detail by means of TSDC techniques (Figs. 1 and 3). At temperature $T = 30°C$ the TPU phase is in the rubbery state while SAN is in the glassy state. The calorimetric glass transition T_g of pure SAN is at 114°C [14], so the corresponding relaxation peak will enter into our frequency window at higher temperatures (Fig. 6). At the temperature of 30°C the secondary γ and β relaxations (Figs. 1 and 2) are located at frequencies higher than 1 MHz and, thus, are not observed in Fig. 5. The dispersion we observe at low frequencies is due to the interfacial MWS polarization mechanism [19]. The motion of space charges within the sample and their trapping at the boundaries (interfaces) in the heterogeneous sample gives rise to this loss peak. This is the mechanism giving rise to the shoulder on the high temperature side of the α TSDC peak in Fig. 1. The slow processes appear at high temperatures in the isochronal plots (TSDC) and at low frequencies in the isothermal plots (DRS). We will discuss the MWS dispersion in more detail below.

Fig. 6 shows ε'' (f) spectra for a 10/90% TPU/SAN sample at different temperatures. These results show a main dielectric dispersion whose position and magnitude allows us to relate it to the main glass–rubber transition (α-relaxation) of the SAN rich phase. Support for this interpretation comes from the fact that this peak was observed on pure SAN and on all the blends but not on pure TPU. With increasing temperature the α-relaxation peak shifts to higher frequencies. At high temperatures and low frequencies the high values of ε'' (and ε', not shown here) do not refer to the bulk of the material. They indicate the existence of space charge polarization and free charge motion within the material [24] and are also related to the so-called conductivity current relaxation [13].

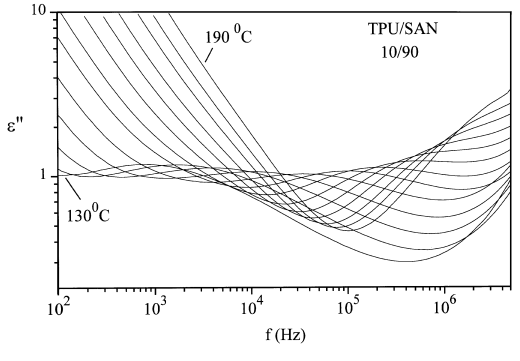

Fig. 6. Dielectric loss ε'' against frequency f, for 10/90% TPU/SAN blend measured at temperatures from $T = 130$ to 190°C in steps of 5°C.

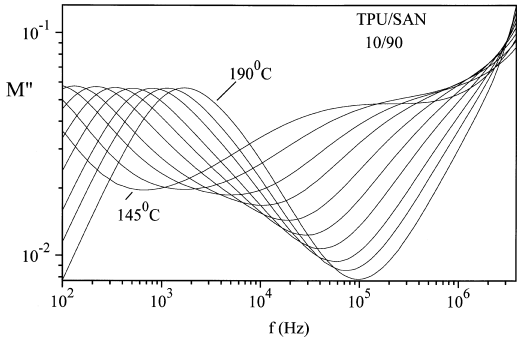

Fig. 7. Imaginary part M'' of the electric modulus M^*, vs frequency f for 10/90% TPU/SAN blend measured at several temperatures in steps of 5°C.

By using the modulus formalism, introduced by Macedo and co-workers [25], we can suppress the large contribution of conductivity to the ε'' (f) plots in Fig. 6. The electric modulus M^*, introduced by analogy to mechanical modulus, is [25]:

$$M* = \frac{1}{\varepsilon*} = M' + iM'' = \frac{\varepsilon'}{\varepsilon'^2 + \varepsilon''^2} + i\frac{\varepsilon''}{\varepsilon'^2 + \varepsilon''^2}. \quad (1)$$

In Fig. 7 we show M'' (f) spectra obtained by transforming the data of Fig. 6 to the M* formalism (Eq. (1). At the temperature $T = 145°C$ we observe only the primary α relaxation of the SAN rich phase of the blend (at $f = 10^4$–10^5 Hz), which shifts to higher frequencies with increasing temperature. At temperatures higher than $T = 160°C$ a new peak appears at low frequencies in Fig. 7 and shifts to higher frequencies with increasing temperature (from about 100 Hz to 2 kHz). This peak corresponds to the contribution of conductivity in ε'' (f) plots in Fig. 6 at low frequencies. The shift of the frequency of maximum M'' with temperature corresponds to the conductivity current relaxation mentioned above [26, 27]. At each temperature the region to the left of the conductivity current relaxation peak is where the charge carriers are mobile over long distances, whereas the region to the right is where the charge carriers are spatially confined to their potential wells. Thus, in the peak region occurs the transition from long range to short range mobility [28]. We will come back to this point later in discussing the ac conductivity plots.

To investigate the effects of blending on the SAN α relaxation we show in Fig. 8, in the more familiar

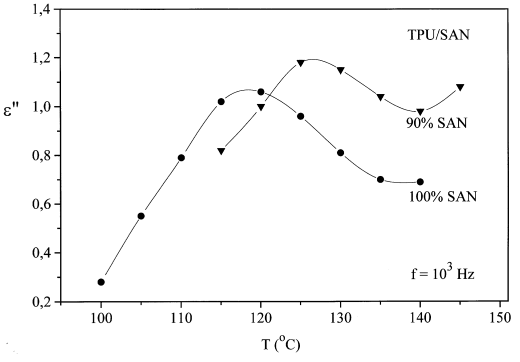

Fig. 8. Dielectric loss ε'' against temperature T at frequency $f = 100$ Hz of pure SAN and 10/90% TPU/SAN blend in the region of the SAN α-peak.

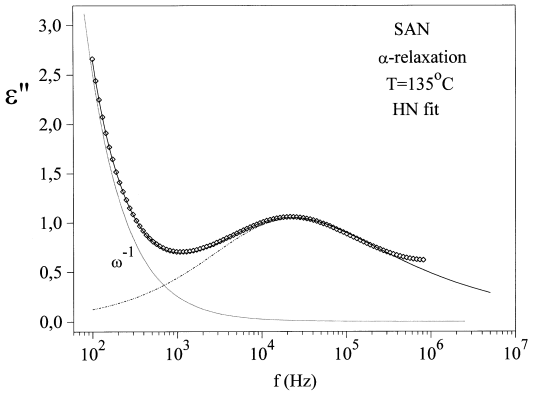

Fig. 9. Dielectric loss ε'' vs frequency f measured at $T = 135$°C for pure SAN sample. The points are experimental results, the lines HN fit [Eq. (2)].

form of isochronal plots, ε'' (T) for pure SAN and for 10/90% TPU/SAN at a fixed frequency of 100 Hz. The points are experimental data obtained from isothermal measurements while the lines are to guide the eye. In agreement with isothermal measurements not shown here we observe that the loss peak associated with the glass–rubber transition of the SAN rich phase shifts to higher temperatures with increasing TPU content, i.e. it is antiplasticized. This result agrees with and completes those shown in Fig. 2 for the secondary γ and β relaxations and is also explained by partitioning between the phases of oligomers in the commercial SAN copolymer.

In order to further analyse quantitatively the data with respect to the temperature dependence and the shape of the response of the α relaxation of the SAN rich phase, the following expression was fitted to the data [29].

$$\varepsilon*(\omega) - \varepsilon_\infty = \frac{\Delta\varepsilon}{[1 + (i\omega\tau)^{1-\alpha}]^\beta} - iA\omega^{-s}. \quad (2)$$

In this equation $\Delta\varepsilon$ is the relaxation strength, $\Delta\varepsilon = \varepsilon_s - \varepsilon_\infty$, where ε_s and ε_∞ the low and high frequency limits of ε', respectively, ω the angular frequency ($\omega = 2\pi f$), $\tau = 1/2\pi f_{HN}$, where f_{HN} is the characteristic Havriliak–Negami (HN) frequency, closely related to the loss peak frequency, f_{max}, α, β the shape parameters describing the shape of ε'' (f) curve below and above the frequency of the peak ($0 < \alpha \leqslant 1$, $0 < \beta \leqslant 1$), A is a constant related to dc conductivity and the exponent s is usually $\leqslant 1$ [30, 31]. In Eq. (2) the first term on the right side is the HN function that describes the dipolar α peak while the second term describes the contribution of conductivity to the spectra. (In the case of more than one dipolar peak a sum of HN functions has to be used. As an example we have shown in Fig. 9 in an ε'' plot the experimental data for the pure SAN sample at $T = 135$°C and the best least squares fit of Eq. (2) to the data. The shape parameters are $\alpha = 0.37$ and $\beta = 0.56$, i.e. the slopes in a log–log plot [29] are $m = (1 - \alpha) = 0.63$ on the low-frequency side and $n = (1 - \alpha)\ \beta = 0.35$ on the high-frequency side. These results suggest a broad and asymmetric distribution of relaxation times. The shape of the α response of the SAN rich phase does not change much with composition. As an example we have shown in Fig. 10 the scaled plot of the α-relaxation peak for pure SAN and two TPU/SAN blends. The shape of the peak does not change much with composition. Bearing in mind that the loss peak becomes broader in miscible polymer blends [32, 33], these results confirm the limited extent of partial miscibility of TPU/SAN blends. The exponent s was found

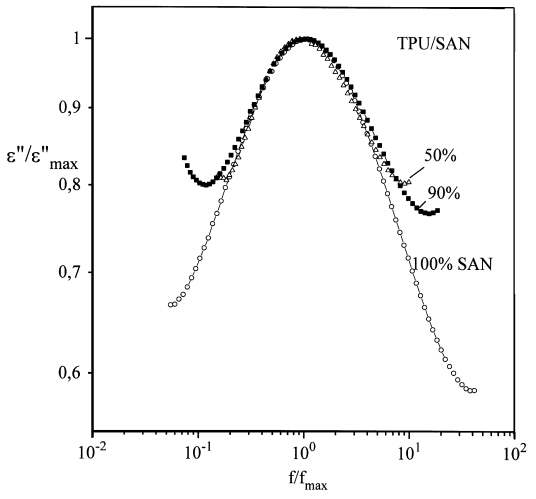

Fig. 10. Scaled plot for the α-relaxation peak for pure SAN and 50% and 90% SAN blends at $T = 155$°C.

to be 1.0, suggesting pure dc conductivity. From the fitting parameter A of the conductivity term we calculate $\sigma = 1.41\times10^{-8}$ S/m, which is in good agreement with the conductivity determined from the plateau values of the a.c. conductivity spectra ($\sigma_{ac} = 1.48\times10^{-8}$ S/m at $f = 10^2$ Hz).

The temperature dependence of $f_{m\varepsilon''}$, and the peak frequency in ε'' (f) plots, of the cooperative molecular motions responsible for the primary α-relaxation mechanism is usually described by the Vogel–Tamman–Fulcher (VTF) equation [31]:

$$f_{m\varepsilon''} = A \cdot \exp[-B/(T - T_0)]. \quad (3)$$

In this equation T is the absolute temperature and T_0 the Vogel or ideal glass transition temperature, A and B are constants. $Lnf_{m\varepsilon''}$ ($1/T$) plots (Arrhenius plots) confirm the VTF-character of the relaxation assigned to the glass transition of the SAN-rich phase and its antiplasticization in the blends. An example is shown in Fig. 11. Extrapolation of the VTF lines to $\tau = 100$ s ($\tau = 1/2\pi f_m$) should give temperatures very close to the calorimetric glass transition temperature [24]. In fact, the values obtained, 75°C for the commercial SAN and 83°C for 10/90% TPU/SAN, are in close agreement with those obtained by DSC [23] and confirm that the α relaxation associated with the glass transition of the SAN-rich phase becomes slower in the blends (Fig. 8).

Results similar to those shown in Figs. 6–11 for the α relaxation of the SAN-rich phase were obtained also with the α relaxation of the TPU-rich phase which is plasticized in the TPU/SAN blends, in agreement with the TSDC results (Fig. 3). To test (also with DRS measurements) the hypothesis that polyurethane and SAN are practically immiscible we show in Fig. 12 Arrhenius plots for the PUR–SAN blends, i.e. the system based on SAN synthesized in the laboratory. In agreement with the TSDC results shown in Fig. 4, we observe that the α relaxation, a well as the secondary γ and β relaxations (the latter less clearly), are slightly antiplasticized in the blend. The fits in Fig. 12 are VTF for the α relaxation and Arrhenius for the secondary relaxations,

$$f_{m\varepsilon''} = f_0 \exp[-E/kT], \quad (4)$$

where f_0, k and E are a constant, Boltzmann's constant and the apparent activation energy, respectively. In addition, scaled plots at different temperatures show that the shape of the SAN α peak does not change much with temperature in the temperature range 130–200°C [33].

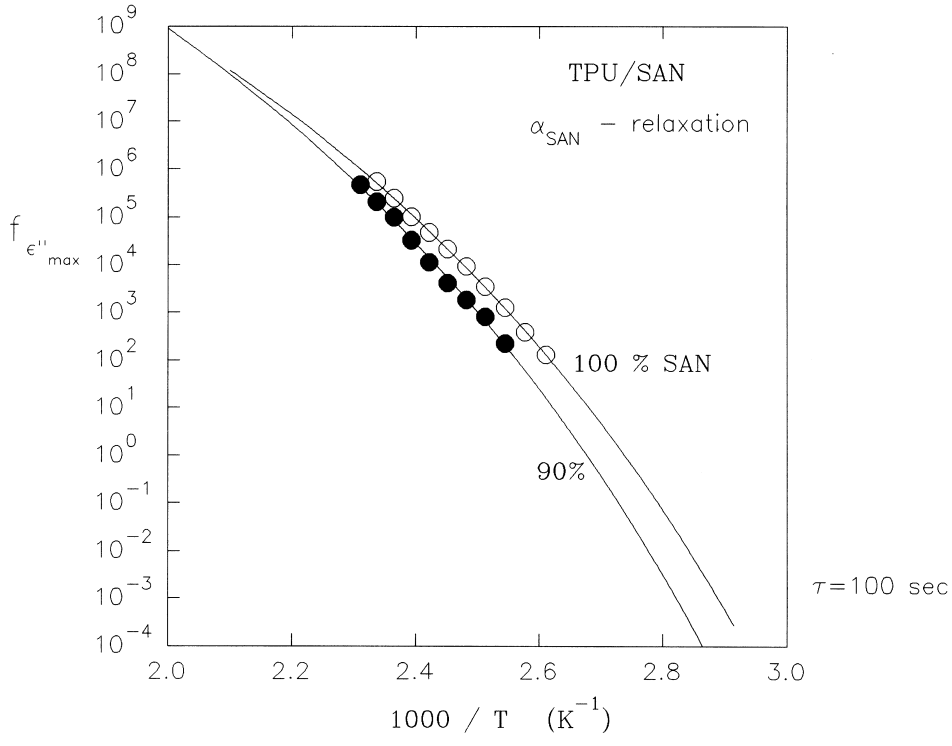

Fig. 11. Arrhenius plots of the ε'' peak frequency $f_{\varepsilon''max}$ for pure SAN and 10/90% TPU/SAN. The lines are VTF fits.

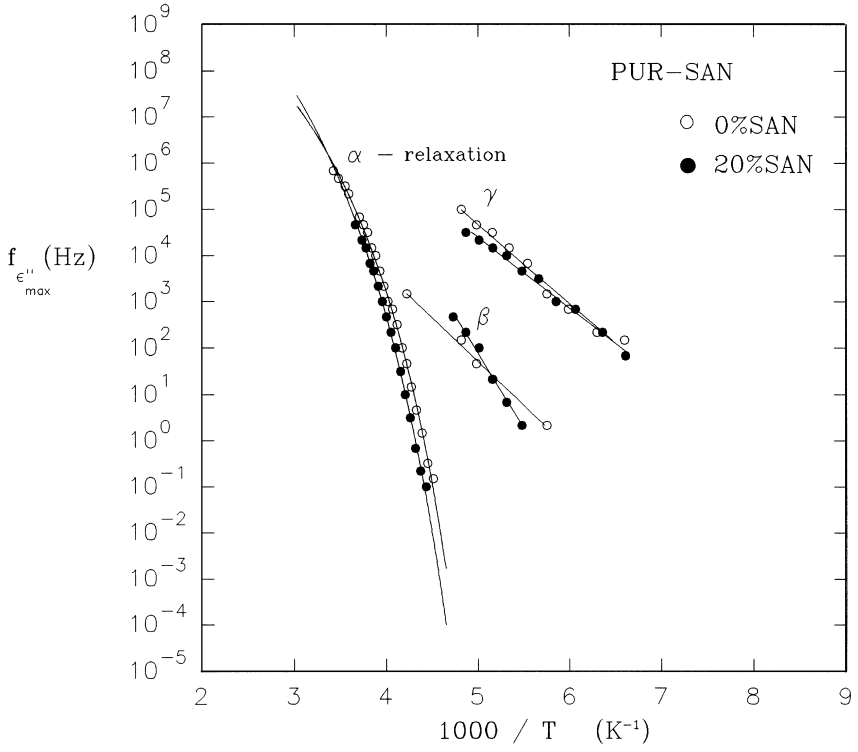

Fig. 12. Arrhenius plots of the ε'' peak frequency $f\varepsilon''$ max for PUR/SAN blends with 0 (o) and 20% () SAN. The lines VTF (α relaxation) and Arrhenius fit (β, γ relaxations).

Arrhenius diagrams of the peak frequency of the imaginary part of the modulus $f_{mM''}$, for the peak related to conductivity, can provide information on charge transport mechanisms within the material [24, 25]. Fig. 13 shows the Arrhenius plots of the $f_{mM''}$ conductivity relaxation peak (a) and of the d.c. conductivity σ_{dc} (b), for pure SAN, pure TPU and TPU/SAN blends. The d.c. conductivity values were determined as the values of a.c. conductivity at low frequencies where the ac conductivity becomes frequency independent [24]. For the pure TPU the solid lines in Fig. 13 are the best least square fittings of the VTF equations:

$$f_{mM''} = A \cdot \exp[-B/(T - T_0)], \tag{5}$$

$$\sigma_{dc} = \sigma_0 \cdot \exp[-B/(T - T_0)], \tag{6}$$

respectively, with A, B, T_0 and σ_0 being constants. The good fits suggest that the charge carrier transport mechanism is governed by the cooperative motion of polymer chain segments. The parameters estimated from the fitting procedure are listed in Table 1.

In terms of the strong–fragile classification scheme, proposed by Angell [34], we used the modified VTF equations to fit our experimental data,

$$f_{mM''} = A' \cdot \exp[-DT'_0/(T - T'_0)], \tag{7}$$

$$\sigma_{dc} = \sigma'_0 \cdot \exp[-DT'_0/(T - T'_0)], \tag{8}$$

respectively. In these equations D is the strength parameter from which we can define also the 'fragility' m parameter: $m = 17 + 580/D$. The parameters D and m describe the deviations from the Arrhenius behaviour [34]. The values of D and m are listed in Table 1. They suggest that the pure TPU is a fragile system.

Contrary to the VTF temperature dependence of $f_{mM''}$ and σ_{dc} in pure TPU, Arrhenius behaviour has

Table 1
Parameters estimated from the fitting procedure of the VTF equation to the conductivity relaxation peak [eqn (5)] and to the dc conductivity values [eqn (6)] for pure TPU

VTF, fragility parameters	M''	σ_{dc}
A (Hz)	1.02×10^{7}	$\sigma_0 = 7.9\times10^{-4}$ S/m
B (K)	843	618
To (K)	157	181
D	5.4	3.4
m	124	188

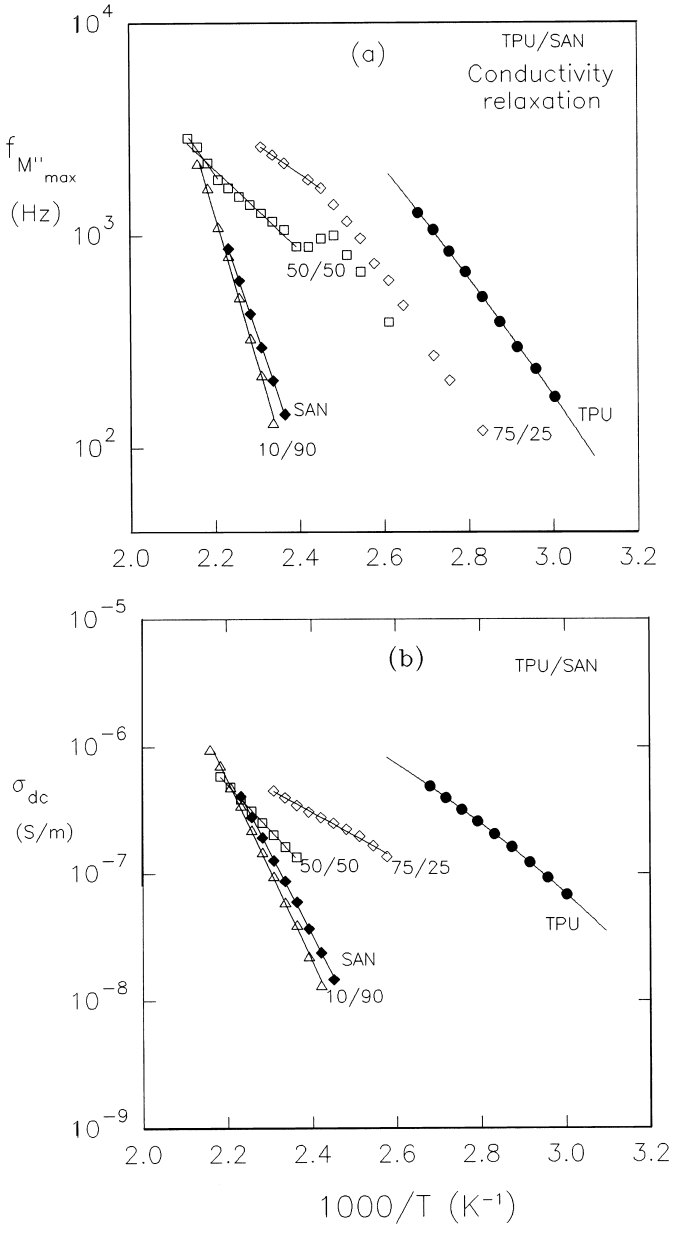

Fig. 13. Arrhenius plots of peak frequency $f_{M''max}$ of the M'' (f) peaks related to conductivity (a) and of dc conductivity σ_{dc} values for TPU/SAN blends (b). The lines for VTF fit for pure TPU and Arrhenius fits for pure SAN and TPU/SAN blends.

been observed in the blends and in pure SAN, described by

$$f_{mM''} = f_0 \cdot \exp[-E/kT], \quad (9)$$

$$\sigma_{dc} = \sigma_0 \cdot \exp[-E/kT], \quad (10)$$

respectively (straight lines in Fig. 12). In these equations f_0 and σ_0 are constants, k is the Boltzmann constant and E the apparent activation energy. The results in Fig. 13 suggest a change of the charge carrier transport mechanism in pure SAN and in the blends compared to pure TPU. The values of activation energy of the conductivity mechanism obtained from the fitting procedure are listed in Table 2. At each composition the values of E obtained within the two formalisms agree fairly well with each other. This

Table 2
The values of activation energy E of the conductivity mechanism obtained from the fitting procedure of the Arrhenius equation to the conductivity relaxation peak [eqn (8)] and to the dc conductivity values [eqn (10)] of pure SAN and TPU/SAN blends

	E (eV)	
TPU/SAN	M''	σ_{dc}
75/25	0.30	0.35
50/50	0.60	0.70
10/90	1.40	1.40
SAN	1.20	1.30

suggests that the M'' peak arises from the dc conductivity mechanism. Within each formalism E is much lower for the 50/50 and the 75/25 TPU/SAN blends than for the 10/90 and the 0/100 samples. We come back to this point later in discussing the implications of our results with respect to the morphology of the blends.

In Fig. 14 we show the frequency dependence of ac conductivity for pure SAN, TPU and three TPU/SAN blends at temperature $T = 30°C$. Similar measurements were performed at several temperatures and were used to obtain the dc conductivity values for constructing the Arrhenius plots in Fig. 13(b). At 30°C the pure TPU phase exhibits a plateau conductivity behaviour in relation to frequency. The blends of 75% and 50% TPU have the same conductivity behaviour indicating similarities in morphology of the blends in this composition range from the point of view of the conductivity mechanism. The shoulder in the frequency range 1–10 Hz, which is observed in TPU and in the blends but not in pure SAN and which increases in magnitude with increasing TPU content, indicates the existence of an additional mechanism. This mechanism is that of the interfacial MWS polarization observed in Fig. 5.

To further analyse and discuss the conductivity current relaxation and the MWS polarization we used the modulus formalism. Fig. 15(a) shows the imaginary part M'', against a frequency for TPU/SAN blends measured at $T = 30°C$. For pure TPU two peaks are observed, located at about 0.1 and 2 Hz, respectively. The low frequency peak at about 0.1 Hz is due to the conductivity current relaxation and is located in the frequency region of transition from frequency independent to frequency dependent conductivity (Fig. 14). The higher frequency peak, at about 2 Hz, is attributed to interfacial MWS polarization (Fig. 5), due to accumulation of charge carriers at the interface between hard and soft segments phase [10]. In the blends 75/25, 50/50, 10/90 TPU/SAN we observe only the MWS peak, due to the interfacial polarization mechanism. The magnitude of the peak (which is absent in pure SAN) is lower in the blends, whereas its frequency position does not change much with composition. These results show that it is the inhomogeneous nature of the TPU component (separation into hard and soft segments phase) which causes the MWS polarization. The low frequency peak at about 0.1 Hz is not present in the blends. It has obviously shifted to lower frequencies outside the range of measurements, in agreement with the results shown in Fig. 13(a) (antiplasticization of the M'' peak in the blends compared to TPU) and in Fig. 14 (no dc conductivity plateau at this temperature).

In order to investigate the shape of the MWS peak in TPU and in the blends and of the conductivity current relaxation in TPU we have fitted the HN expression for a single peak:

$$M* - M_\infty = \frac{\Delta M}{[1 + (i\omega\tau)^{1-\alpha}]^\beta}, \tag{11}$$

to the data obtained with the blends and a sum of two HN terms to the data obtained with TPU. In Eq. (11) $\Delta M = M_\infty - M_0$, where M_∞ and M_0 are the high and low frequency limits of M', respectively, ω the angular frequency ($\omega = 2\pi f$) and α and β shape parameters describing the shape of M'' (f) curve below and above the frequency of the peak ($0 < \alpha \leqslant 1$, $0 < \beta \leqslant 1$). The results of fitting the TPU data are shown in Fig. 15(b) and the corresponding HN parameters are listed in Table 3. The shape parameters α and β are similar for the two peaks, reflecting the fact that the same microscopic mechanism, namely charge transport, gives rise to the two peaks. We would like to note here that at higher temperatures the conductivity current relaxation peak dominates and only one peak is observed in the M'' plots.

In the blends, the results of fitting show that the MWS peak is broader than in TPU indicating a broader distribution of relaxation times of the inter-

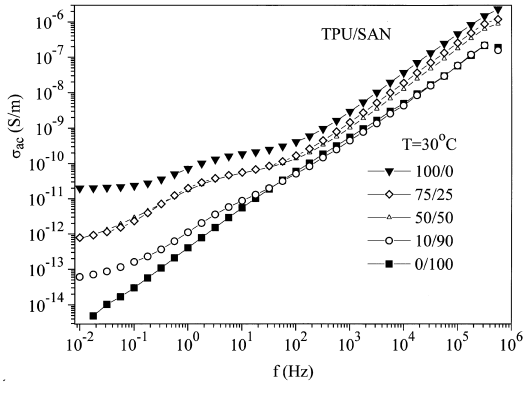

Fig. 14. ac conductivity σ_{ac} as a function of frequency f measured at $T = 30°C$ for TPU/SAN blends.

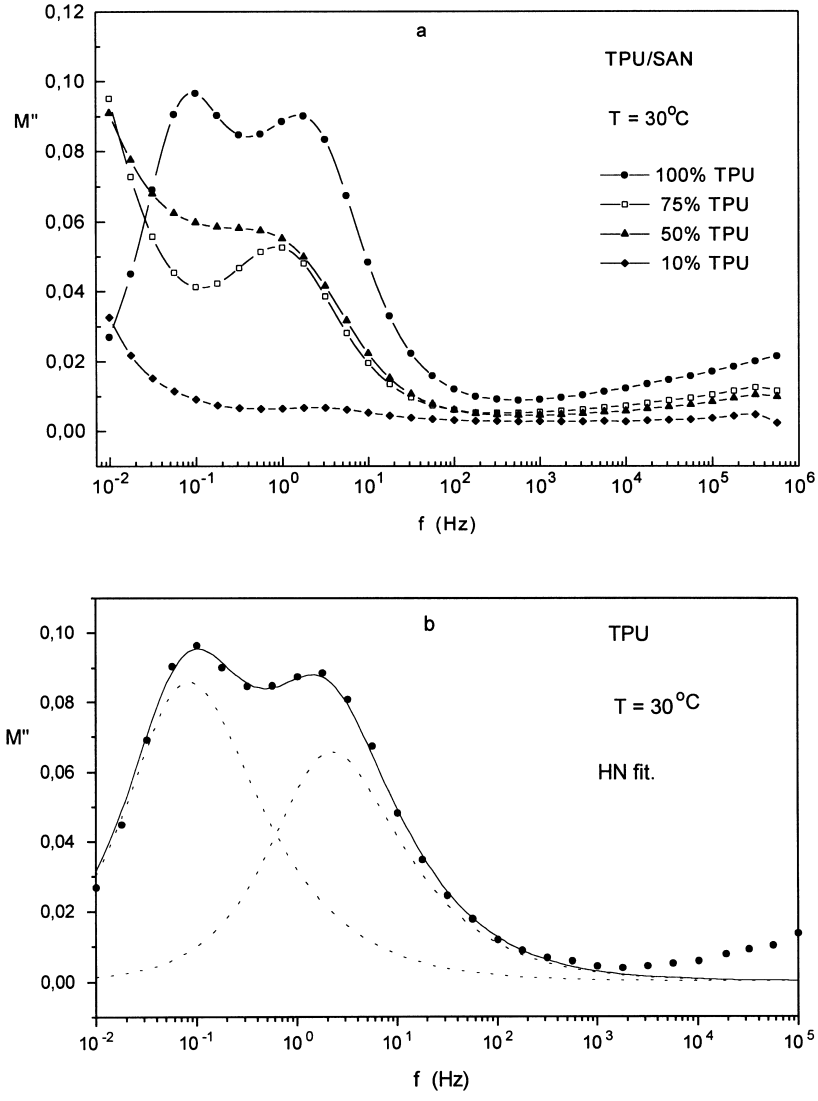

Fig. 15. (a) Imaginary part M'' of electric modulus M^* for TPU/SAN blends measured at $T = 30°C$ (b) HN fit to the M″ (f) spectra for TPU (solid line) and the two components (single HN peaks) of the whole spectra fit (dashed lines).

Table 3
Havriliak–Negami parameters of the conductivity current relaxation M'' (f) peak and of the MWS peak in TPU estimated from fitting procedure of the HN Eq. (11) to the data

HN parameters	Conductivity relaxation peak	MWS peak
$\Delta M'$	0.24	0.18
α	0.12	0.10
β	0.70	0.67
f_0 (Hz)	0.06	1.6

facial polarization mechanism. With respect to morphology these results suggest a diversity in the topology of conducting paths and of interfaces in the blends. For the blends 75/25 and 50/50 TPU/SAN the shape parameters have practically the same values, indicating similar morphology in these two blends.

Fig. 16 shows the static dielectric permittivity ε_s, obtained as the value of ε' at $f = 100$ Hz, as a function of composition measured at three different temperatures. As expected, at each temperature ε_s increases with increasing TPU content. At the temperatures of

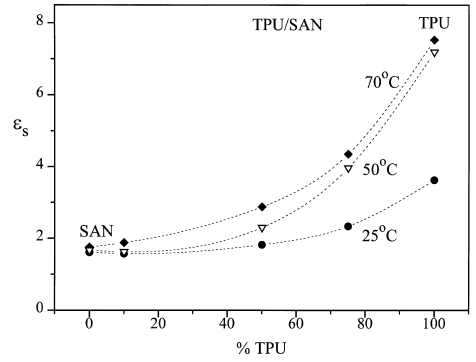

Fig. 16. Static dielectric permittivity ε_s as a function of TPU/SAN blends composition measured at different temperatures.

measurements in Fig. 16, SAN is in the glassy phase whereas TPU is rubbery. A striking feature in Fig. 16 is the significant increase of ε_s at 50°C compared to 25°C observed in TPU and in TPU rich blends. This increase can be explained by the melting of the CAPA crystalline phase at 40°C observed by DSC in our samples [23] and in poly(*g*-caprolactone)-*g*-poly(methyl methacrylate) co-polyurethanes [35].

To further investigate changes in the morphology induced by blending and by temperature increases we have shown in Fig. 17 the dielectric permittivity ε' measured at $f = 10^4$ Hz as a function of temperature for the different compositions studied. The frequency of measurements, 10^4 Hz, should be low enough to include in ε' all the polarization mechanisms and high enough to exclude effects due to dc conductivity. At about 40°C we observe a step in ε' for the samples with TPU content more than 50%. As discussed above on the basis of Fig. 16 we attribute this step to melting of the crystalline soft segments phase of TPU [23, 35]. This step is very steep, indicating that DRS is a sensitive tool to investigate such effects in complex polymeric systems. For comparison, the melting of the crystalline soft segments phase in poly(*g*-caprolactone)-*g*-poly(methyl methacrylate) co-polyurethanes at 40°C (DSC) is observed in dynamic mechanical thermal analysis measurements as a gradual decrease of the shear modulus between 0 and 50°C [35]. The step in ε' at about 40°C is not observed with the 10/90 TPU/SAN blend and it is rather small in the 50/50 and 75/25 TPU/SAN blends compared to pure TPU. It follows that the degree of crystallinity of the soft segments TPU phase is greatly reduced in the blends. In the samples with 50 and 75% TPU we observe a gradual increase of ε' with temperature and a step in ε' at about 60–70°C, respectively. We attribute these changes, which are not observed with the 100% TPU sample, to the glass–rubber transition of the hard segments of TPU, in agreement with DSC results in ref. [23] and in similar [35] samples. This transition is not observed with the pure TPU component, in agreement with DSC results [23]. It follows that the addition of SAN to TPU promotes phase separation into a hard segments phase and a soft segments phase of TPU. These results are in agreement with those of wide angle X-ray diffraction (WAXD) and scanning electron microscopy (SEM) measurements on TPU/SAN blends [9] and of dynamic mechanical analysis (DMA) on PUR/SAN blends [14]. The increase in ε' in the temperature region of 120–150°C, which becomes less pronounced with decreasing SAN content of the blends, is attributed to the glass to rubber transition of the SAN rich phase. The increase in ε' at temperatures higher than about 150°C is difficult to attribute to specific morphological changes. In the TPU containing blends they may be at least partly due to the break-up of hard-segment domains of TPU [35]. Conductivity effects are also likely to contribute to ε' at these high temperatures.

In Fig. 18 we show the composition dependence of the dc conductivity values of the TPU/SAN blends at

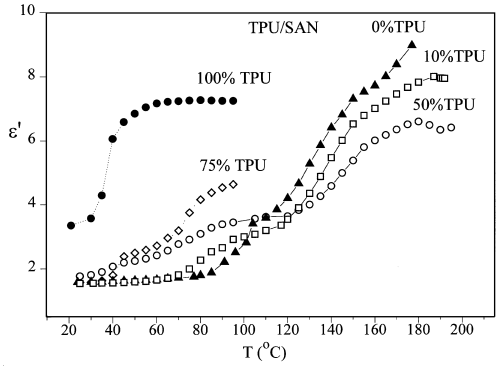

Fig. 17. Dielectric permittivity ε' measured at frequency $f = 10^4$ Hz vs temperature T for the different TPU/SAN compositions studied.

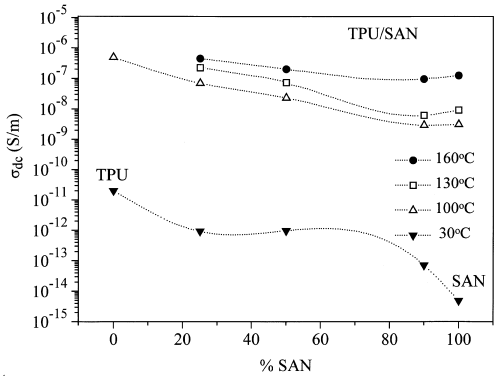

Fig. 18. Dc conductivity values σ_{dc} against composition for the TPU/SAN blends measured at different temperatures.

different temperatures. The values were obtained from the frequency independent limits of the σ_{ac} values (at $f = 0.01$ Hz for $T = 30°C$ and $f = 100$ Hz for the other temperatures). It is observed that the pure TPU sample is more conductive than SAN at 30°C. At this temperature the TPU phase is in the rubbery state whereas the SAN phase is in the glassy state. In the blends the dc conductivity becomes lower compared with that of the pure TPU phase. The dc conductivity has similar values for the 75/25 TPU/SAN and 50/50 TPU/SAN, which is by a factor of about 25 lower than in TPU, suggesting similar morphology in these blends. It is interesting to note that the same conclusion was drawn from the investigation of the MWS interfacial polarization peak in Fig. 15. Moreover, the results in Fig. 13 suggested a change of the conductivity mechanism from a VTF type one in TPU to an Arrhenius-type one in the blends and in SAN. In view of this change of mechanism and bearing in mind the well established fact that VTF-type conductivity mechanisms are characterized by significantly higher values of dc conductivity than expected for diffusion-controlled ones [36], it is not surprising that σ_{dc} is by a factor of about 25 lower in 75/25 and in 50/50 TPU/SAN blends than in pure TPU. In addition, the values of activation energy E of both d.c. conductivity and conductivity current relaxation were found to be much lower for the 75/25 and the 50/50 TPU/SAN blends than for the 10/90 and the 0/100 samples (Fig. 13 and Table 2). These results suggest that TPU is the continuous phase in the 75/25 and the 50/50 TPU/SAN blends and SAN in the 10/90 blends. It is interesting to note that mechanical measurements on TPU/SAN blends indicate that the phase inversion between continuous and discontinuous phase occurs at approximately 50 wt% SAN in the blend [37]. Thus, the conductivity changes in Fig. 18 are related to morphology changes. At higher temperatures ($T \geqslant 100°C$) the dc conductivity composition reflects less clearly the morphology of the material compared to the 30°C measurements. This is because at these temperatures both phases are in the rubbery state, which is characterized by increased conductivity as a result of increased chain mobility.

4. Conclusions

Summarizing, we have investigated the mechanisms of molecular mobility in blends of thermoplastic polyurethanes (TPUs) and styrene–acrylonitrile (SAN) copolymers by means of dielectric techniques in wide ranges of frequency and temperature. For the preparation of these blends commercial SAN was used, which contains low molecular weight oligomers [21, 22]. For comparison, some measurements were performed with a second blend, PUR/SAN, consisting of cross-linked polyurethanes and SAN copolymers. In this second blend SAN was synthesized in the polyol and was free of oligomers [14]. In addition, the TPU/SAN blends were cast from DMF solution, whereas the PUR/SAN blends were prepared solvent free.

Our results show that the local secondary γ and β mechanisms of TPU are plasticized, whereas those of SAN are antiplasticized in the TPU/SAN blends (Fig. 2). In addition the α mechanism associated with the glass transition of the soft segments phase of TPU is plasticized in the blends (Fig. 3). The α mechanism associated with the glass transition of SAN is antiplasticized in the TPU/SAN blends (Figs. 8 and 11), whereas the shape of the corresponding loss peak does not change much with composition (Fig. 10). These results cannot be explained based on phase mixing. A plausible explanation consistent with all the results obtained with the TPU/SAN blends and with literature data [21, 22] is that the observed plasticizing effects on TPU and the antiplasticizing ones on SAN result from partitioning between the phases of oligomers in the commercial SAN copolymer. Support for this explanation comes from preliminary measurements on the PUR/SAN blends (Figs. 4 and 12). They show that the PUR γ, β and α mechanisms are slightly antiplasticized, whereas the α mechanism of SAN is not affected much by blending (not shown here). The conclusion to be drawn from all these results is that polyurethanes and SAN are only to a limited extent miscible.

The investigation of conductivity effects provides significant information on the morphology at the mesoscopic level as conductivity is related to transport of charges over microscopic to macroscopic distances, depending on the frequency of measurements. In general, the dc conductivity (Fig. 18) and the ac conductivity (Fig. 14) decrease with increasing SAN content in the TPU/SAN blends. The temperature dependence of dc conductivity and of the conductivity current relaxation, studied in the modulus formalism, is described by the VTF equation for the pure TPU component (Fig. 13). Within the fragility scheme [26] TPU is a fragile system (Table II–I).

The results in Fig. 16 show that DRS is a sensitive tool to monitor the melting of the crystalline soft segments of TPU phase at about 40°C. In addition, the investigation of dielectric effects in the temperature region of T_g of the hard segments phase of TPU (60–70°C) provides strong evidence that the addition of SAN to TPU promotes the separation into hard and soft segment phases of TPU (Fig. 17). In view of the negligible effects of SAN on Tg of the soft segments phase of PUR in the PUR/SAN blends (Figs. 4 and 12), this promotion of phase separation should arise from interaction of SAN with the hard segments of polyurethanes. According to ref. [9], interaction is pre-

dominantly determined by polarity and mobility of the SAN chains.

Acknowledgements

The authors would like to thank Dr M. Ulcnik, University of Maribor, for the preparation of the blends.

References

[1] Schneider HA, Di Marzio EA. Polymer 1992;33:3453–61.
[2] Roland CM, Ngai KL. J Rheol 1992;36:1691–706.
[3] Adachi K, Wada T, Kawamoto T, Kotaka T. Macromolecules 1995;28:3588–96.
[4] Sauer BB, Avakian P, Cohen GM. Polymer 1992;33:2666–71.
[5] Shiao KR, Wang HH. J Mat Sci Lett 1991;10:348–51.
[6] Paul DR, Newman S, editors. Polymer Blends, Vol. 1. New York: Academic Press, 1978.
[7] Iskandahr M, Tran C, McGrath JE. Polymer Preprints of American Chemical Society 1985;24:126–9.
[8] Ratzsch M, Handel G, Pompe G, Meyer E. J Macromolecular Sci A 1990;27:1631–55.
[9] Zerjal B, Musil V, Smit I, Jelcic Z, Malavasic T. J App Poly Sci 1993;50:719–27.
[10] Spathis G, Kontou E, Kefalas V, Apekis L, Christodoulides C, Pissis P, Ollivon M, Quinquenet S. J Macromolecular Sci–Phy 1990;B29:31–48.
[11] Migahed MD, Ishra M, El–Khodary A, Fahmy T. Poly Test 1993;12:335–49.
[12] Moynihan CT, Boesch LP, Laberge NL. Phys Chem Glass 1973;14:122–5.
[13] Jain H, Ngai KL. In: Ngai KL, Wright GB, editors. Relaxations in Complex Systems. Washington, DC: Naval Research Laboratory, 1984. p. 221–7.
[14] Mitzner E, Goering H, Becker R. Die Angewandte Makromolekulare Chem 1994;220:177–88.
[15] van Turnhout J. In: Sessler GM, editors. Thermally stimulated discharge of electrets, Topics in Applied Physics. Electrets. Berlin: Springer, 1980. p. 81–215.
[16] Pissis P, Anagnostopoulou–Konsta A, Apekis L, Daoukaki–Daimanti D, Christodoulides C. J Non-cryst Sol 1996;131–133:1174–81.
[17] Kyritsis A, Pissis P, Gomez Ribelles L J, Monleon Pradas M. J Poly Sci Poly Phys,32:1001–8.
[18] McGrum NG, Read BE, Williams G, editors. Anelastic and Dielectric Effects in Polymeric Solids. New York: Wiley, 1967.
[19] Hedvig P. Dielectric Spectroscopy in Polymers. Bristol: Adam Hilger, 1977.
[20] Pissis P, Apekis L, Christodoulides C, Niaounakis M, Kyritsis A, Nedbal J. J Poly Sci Polymer Phys 1996;34:1529–39.
[21] Schellenberg J, Hamman B. E Poly J 1993;29:727–30.
[22] Callaghan TA, Takakuwa K, Paul DR, Padwa AR. Polymer 1993;34:3796–808.
[23] Ulcnik M, Zerja B, Malavasic T. Therm Acta 1996;276:175–87.
[24] Kyritsis A, Pissis P, Grammatikakis J. J Poly Sci Polymer Physics 1995;33:1737–50.
[25] Macedo PB, Moynihan CT, Bose R. Phys Chem Glas 1972;13:171–79.
[26] Angell CA. Mat Chem Phys 1989;23:143–69.
[27] Jain H, Ngai KL. In: Ngai KL, Wright GB, editors. Washington: Naval Research Laboratory, 1984. p. 221–7.
[28] Patel HK, Martin SW. Physical Review B. 45. p. 10292–300, 1992.
[29] Schoenhals A, Kremer F, Schlosser E. Phys Rev Let 1991;67:999–1002.
[30] Boese D, Kremer F. 1990;24:829–35.
[31] Hofmann A, Kremer F, Fischer EW, Schoenhals A. In: Richert R, Blumen A, editors. Disorder Effects on Relaxational Processes. Berlin: Springer, 1994. p. 309–31.
[32] McGrath KJ, Rolland CM. J Non-crystalline Solids 1991;172–174:891–6.
[33] Katana G, Fischer EW, Hack Th, Abetz V, Kremer F. Macromolecules 1995;28:2714–22.
[34] Angell CA. J Non-cryst Sol 1991;131–133:13–31.
[35] Rimmer S, George MH. Polymer 1994;35(26):5782–4.
[36] Polak AJ. Ionically conductive polymers. In: Margolis JM, editor. Conductive polymers and plastics. New York: Chapman and Hall, 1989. p. 41–90.
[37] Zerjal B, Musil V, Jelsic Z, Smit I, Malavasic T. International Polymer Processing, VII. Munich: Hanser, 1992. p. 123–5.